ISSN 0038-0946, Solar System Research, 2018, Vol. 52, No. 7, pp. 691–698. © Pleiades Publishing, Inc., 2018.
Original Russian Text © I.A. Sobolev, 2017, published in Vestnik NPO imeni S.A. Lavochkina, 2017, No. 4, pp. 108–115.

Analysis of Design Characteristics of Snake-Type Atmospheric Probes (Vetrolets) for Studying the Atmosphere of Venus

I. A. Sobolev*, **

OOO Sputnix, Skolkovo, Moscow, 121205 Russia

**e-mail: i.sobolev@sputnix.ru*

***e-mail: sw72@mail.ru*

Received July 28, 2017

Abstract—In Russia, work aimed at designing a spacecraft for the long-term exploration of Venus is currently underway as part of the VENUS-D project. The R&D work proposes the concept of a snake-type atmospheric probe intended for exploring the atmosphere of Venus. This article describes the principles of flight, considers the main design features and engineering characteristics of the probes, and provides recommendations for engineering solutions.

Keywords: VENUS-D project, atmosphere of Venus, research of Venus, vetrolet, atmospheric probe, parachute

DOI: 10.1134/S0038094618070183

INTRODUCTION

The practical exploration of Venus has brought to light the relevance and expediency of creating probes intended for long-term work in the planet's atmosphere and exploration of both the atmosphere and surface of Venus. On June 11 and 15, 1986, as part of the VEGA project, aerostatic probes were launched for the first time in the world's history (Vaisberg, 2016). The aerostats completed the flight's fully planned program and confirmed the practical feasibility of the chosen concept.

At the same time, the potential of aerostatic probes is limited by emerging technical issues (in particular, by limited battery capacity and the gas-permeable balloon shell) as well as the properties of Venus's atmosphere, primarily the high speed of its circulation and dynamic instability. On the other hand, the high cost of organizing an expedition and the value of exploration data require extending the probe's active life; in this respect, this leads to new design and even conceptual solutions.

Probe Configuration

The first brief description of the concept of a vetrolet probe is given in (Vorontsov et al., 2012). The utilization of a gliding probe of this type was also considered as part of the unimplemented VESTA project (Lemeshevskii et al., 2017): in that project the active design life of the probe was one month, the exploratory equipment weight was 20 kg, and the flight altitude was 40 to 50 km (Vorontsov et al., 2012).

The vetrolet probe is an aerodynamic engine-free airborne vehicle for exploring the atmosphere and surface of Venus. The probe is driven by the wind, the lifting force is generated by the aerodynamic quality of the airfoil. The design parts of the probe are (Fig. 1):

—The airfoil intended for generating the lifting and the drift force.

—Braking parachute for generating the braking force to ensure the girtline tension and the operation of the airfoil.

—Nacelle for mounting the instrumentation.

—Girtline for the mechanical connection between the nacelle and the airfoil.

The general design relations of the snake-type probe were given in (Vorontsov et al., 2012). The probe embodies two possible concepts with differently designed airfoils. In the first case, the airfoil has a soft (para-glider) or a semirigid (hang-glider) design; in the second case, it has a rigid design (glider).

The soft and semirigid configurations have such strengths as low weight and a simply designed and deployable airfoil. The weaknesses are the risk of sling entanglement during release, the risky impact of long-term factors of space travel on the airfoil when folded, the possible rupture of the airfoil during release, and complicated flight control.

The strengths of the rigid member are better structural resistance to space-travel factors, absence of slings, better structural strength and rigidity, the possibility of installing the control system right on the airfoil, the possibility of choosing the form of the airfoil

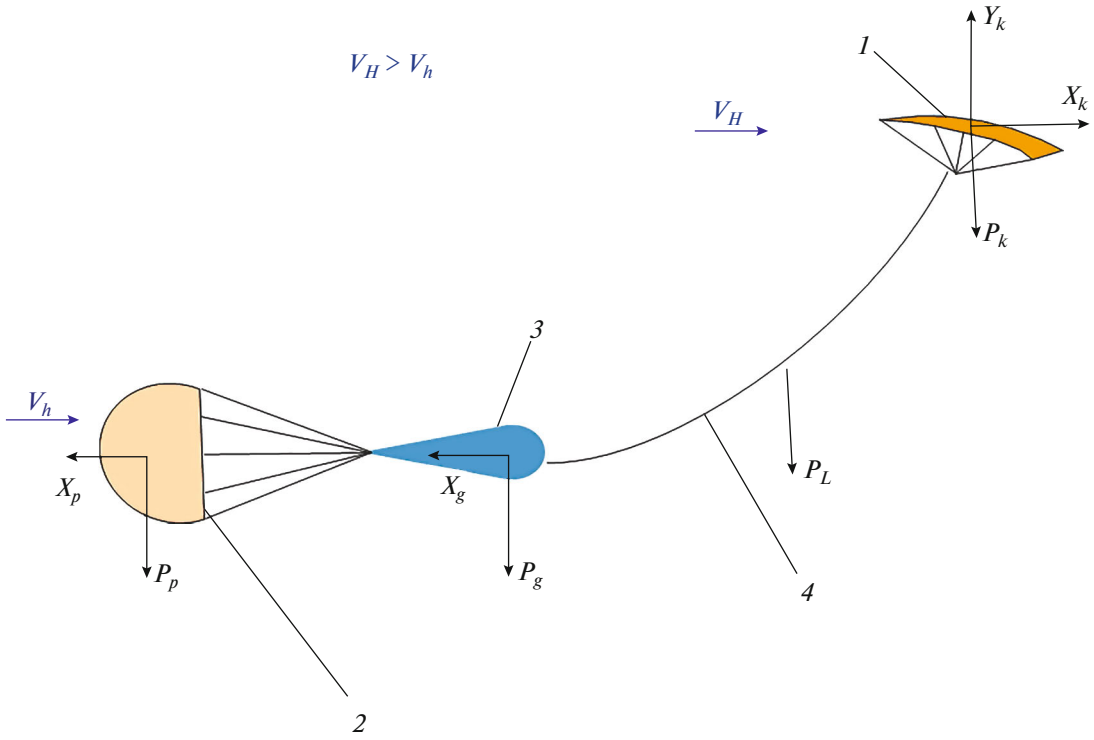

Fig. 1. Forces that affect the vetrolet probe: *1*, airfoil; *2*, braking parachute; *3*, nacelle; *4*, girtline.

section and ensuring better aerodynamic performance. The airfoil intended for overcloud flights may have a propulsion plant for maintaining (as required) altitude during flight and photovoltaic sensor panels for battery recharging. The weaknesses of this design are a heavier airfoil and certain complex aspects of deploying it in the flight configuration.

Main Design Relations

During drift, the carrier is at height H, where the wind speed is V_H; the nacelle and the braking parachute are at height h, where the wind speed is V_h. That said, $H > h$ and $V_H > V_h$. The probe as a rigid whole travels by action of the wind at speed V_c and $V_h < V_c < V_H$. Thus, the air flow rates over the airfoil and the nacelle and the braking parachute are $w_H = V_H - V_c$ and $w_h = V_c - V_h$, respectively.

In the simplest version, the steady flight of the probe in the atmosphere is described using a system of two equations. The first equation expresses the equality of the resistance forces of the airfoil and the braking parachute with the nacelle:

$$C_{Xk}\rho_H \frac{(V_H - V_c)^2}{2} S_k = (C_{Xp}S_p + C_{Xg}S_g)\rho_h \frac{(V_c - V_h)^2}{2}, \quad (1)$$

where V_h is the wind speed at the nacelle's altitude, m s^{-1};

V_H is the wind speed at the airfoil's altitude, m s^{-1};

V_c is the probe velocity, m s^{-1};

ρ_h is the atmospheric density at the nacelle's altitude, kg m^{-3};

ρ_H is the atmospheric density at the airfoil altitude, kg m^{-3};

C_{Xp} is the parachute resistance factor;

S_p is the parachute area, m^2;

C_{Xg} is the nacelle resistance factor;

S_g is the nacelle midsection area, m^2;

C_{Xk} is the airfoil resistance factor;

S_k is the airfoil area, m^2.

The second equation expresses the equality of the airfoil's lifting force and the total weight of the system:

$$C_{Yk}\rho_H \frac{(V_H - V_c)^2}{2} S_k = (m_k + m_l + m_g + m_p) g_a, \quad (2)$$

where C_{Yk} is the airfoil lifting force factor;

m_k is the airfoil weight, kg;

m_l is the girtline weight, kg;

m_g is the nacelle weight, kg;

m_p is the parachute system weight, kg;

g_a is the acceleration due to gravity, m s^{-2}.

Table 1. Possible characteristic variation ranges of the airfoil

Design	Aerodynamic quality	Load on area, kg/m^2	Unit weight, kg/m^2
Soft (paraglider)	5–7	2.2–3.8	~0.25
Semi-rigid (hang-glider)	11–12	10–11	1.5–3
Rigid (glider)	15–35 and more	15–30 and more	8–10and more

The formula found from equations (1) and (2) is

$$\frac{1}{k} = \frac{(C_{Xp}S_p + C_{Xg}S_g)\rho_h (V_c - V_h)^2}{2(m_k + m_l + m_g + m_p) g_a},$$

where $k = C_{Yk}/C_{Xk}$ is the airfoil aerodynamic quality,

or, considering that $V_c > V_h$,

$$V_c = V_h + \sqrt{\frac{2(m_k + m_l + m_g + m_p) g_a}{k(C_{Xp}S_p + C_{Xg}S_g)\rho_h}}. \quad (3)$$

According to the analysis of (3):

—The increased aerodynamic quality of the airfoil entails the reduced value of the expression under the root sign and, therefore, decreases the resultant probe speed V_c at given h and V_h. Since the altitude of the probe is maintained in the atmosphere by requiring that $V_H > V_c$, and the wind speed increases as the altitude increases, the altitude H required for the airfoil will be lower at lower V_c and the required girtline length shorter, which makes the probe more reliable (entanglement becomes less likely) and somewhat lighter.

—The same effect for an airfoil with a fixed aerodynamic quality can be attained by increasing the braking parachute resistance $C_{Xg}S_g$, reducing the overall system weight, or lowering the nacelle altitude h.

The airfoil area is found as

$$S_k = \frac{m_\Sigma}{p_s},$$

where $m_\Sigma = m_k + m_l + m_g + m_p$ is the overall probe weight; p_s is the specific load on the airfoil area, kg m^{-2}.

In the case the altitude changes and, consequently, the airflow speed and atmospheric density change as well, the variable quantities on the right-hand side will be m_k and m_l that can be represented as

$m_k = m_{spk}S_k$, where m_{spk} is the specific airfoil weight, kg m^{-2};

$m_l = m_{spl}L_l$, where m_{spl} is the specific girtline weight, kg m^{-1}; and L_l is the girtline length, m.

Then, the result we obtain from (2) for the flow rate over the airfoil is

$$V_H - V_c = \sqrt{\frac{2p_s g_a}{C_{Yk}\rho_H}}. \quad (4)$$

As may be seen from (4), the increased load on the wing increases the required speed of the flow around the airfoil $V_H - V_c$ or increases V_H at fixed V_c, i.e., increases the altitude of the airfoil and, consequently, the girtline length.

According to the analysis of terrestrial alternatives, the airfoil aerodynamic quality, wing loading, and specific weight can vary in the ranges indicated in Table 1.

How the Braking Dome Works

The braking dome work schema is shown in Fig. 2.

It follows from the schema that the braking dome is functional when the pressure difference on its outer and inner surface is $\Delta p = p_1 - p_2$ and exceeds the specific dome fabric weight $m_{sp}g_a$ (otherwise, the upper edge will sag and the dome collapse). According to (Lobanov, 1965), Δp is related to the fast pressure head on the dome $q = (\rho_h w)/2$ via equation $\Delta p = 1.6q$. Thus we have

$$1.6\frac{\rho_h w_h}{2} > m_{sp}g_a$$

or

$$w_h > \sqrt{\frac{m_{sp}g_a}{0.8\rho_h}} = w_{h\min}. \quad (5)$$

Given the specific parachute weight is 220 g m^{-2} and referring to the distribution of wind speeds by altitude given in Table 2, we find the minimal speeds of the flow over the braking dome that are included in Fig. 3.

Thus, the minimal necessary speed w_h of the airflow around the braking dome increases with increasing nacelle altitude and the corresponding reduction in the atmospheric density.

Table 2. Accepted model of wind speed distribution by altitude

Altitude, km	Wind speed, m s^{-1}	Wind speed gradient, m s^{-1} km^{-1}
45	52	3
61	100	8
65	132	–

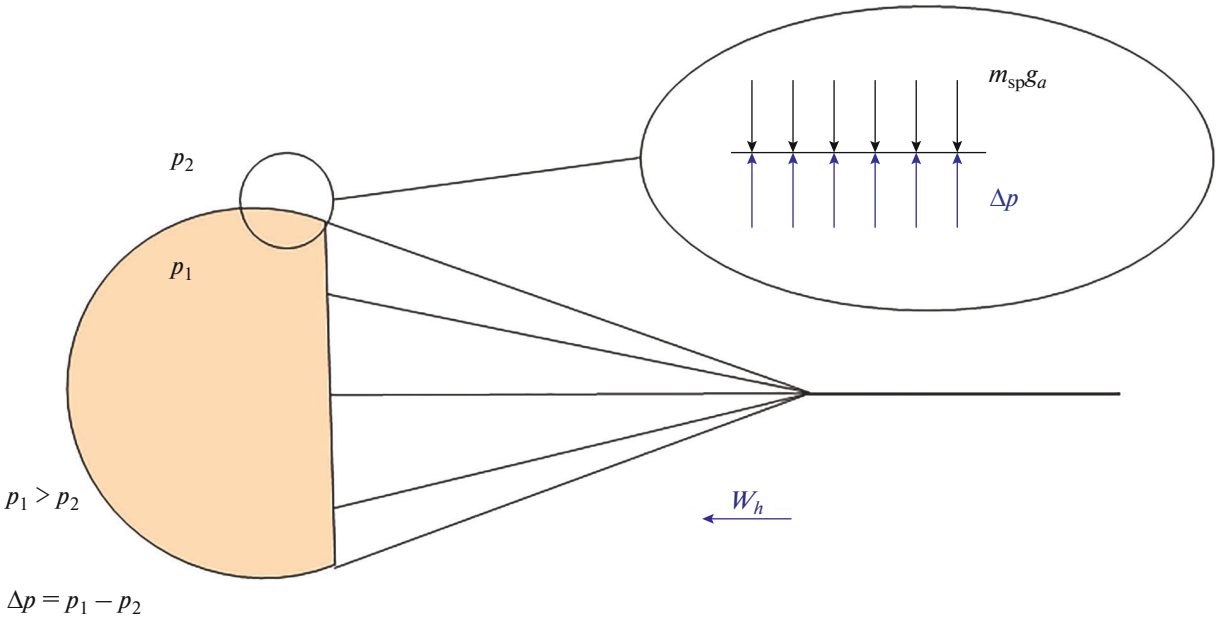

Fig. 2. Brake dome operation pattern.

Noting that $w_h = V_c - V_h$ and considering (3) and (5) together, we have

$$\sqrt{\frac{2(m_k + m_l + m_g + m_p)g_a}{k(C_{Xp}S_p + C_{Xg}S_g)\rho_h}} > \sqrt{\frac{m_{sp}g_a}{0.8\rho_h}}.$$

Assuming that the braking parachute resistance factor C_{xp} applies to its full area S_p, which means that $m_{sp}\, S_p = m_p$ (in the case the contribution of the sling weight to the parachute weight is much less significant than that of the dome), we arrive at the following equation by transformations:

$$m_p < \frac{1.6(m_k + m_l + m_g)}{k\left(C_{Xp} + C_{Xg}\dfrac{S_g}{S_p}\right) - 1.6}$$

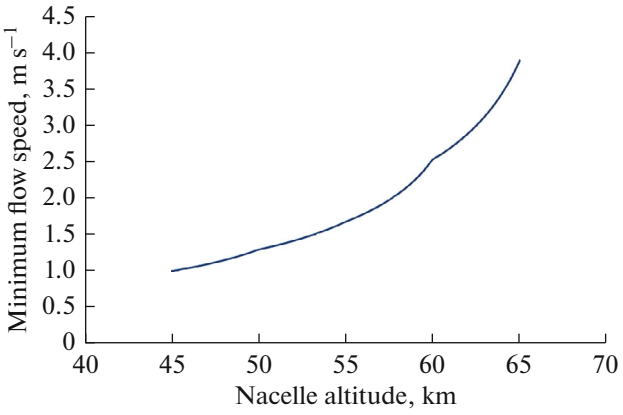

Fig. 3. Minimum speed of the flow over the braking dome.

or

$$k\left(C_{Xp} + C_{Xg}\frac{S_g}{S_p}\right) < 1.6\left(1 + \frac{m_k + m_l + m_g}{m_p}\right). \quad (6)$$

Equation (6) shows the relation between the weight and aerodynamic characteristics of the main parts of the vetrolet probe.

The minimum permissible speed of the flow around the airfoil corresponds to the stall speed is found to be

$$w_{sp} = k_v\sqrt{\frac{2m_\Sigma g_a}{0.85C_{Y\max}\rho_H S_k}}, \quad (7)$$

where $C_{Y\max}$ is the airfoil maximum lifting force factor and k_v is the speed reserve factor.

Thus, the minimum acceptable wind speed V_H at the airfoil altitude at the probe speed V_c found by (3) will be

$$V_{H\min} = V_c + W_{sp}$$

or, taking (3) and (7) into account,

$$V_{H\min} = V_h + \sqrt{\frac{2m_\Sigma g_a}{k(C_{Xp}S_p + C_{Xg}S_g)\rho_h}} + k_v\sqrt{\frac{2m_\Sigma g_a}{0.85C_{Y\max}\rho_H S_k}}. \quad (8)$$

Thus, the minimum wind speed at the airfoil altitude consists of the wind speed at the nacelle altitude, the air speed around the braking parachute, and the airfoil stall speed. Summand one is determined by the required altitude of the nacelle with the instrumenta-

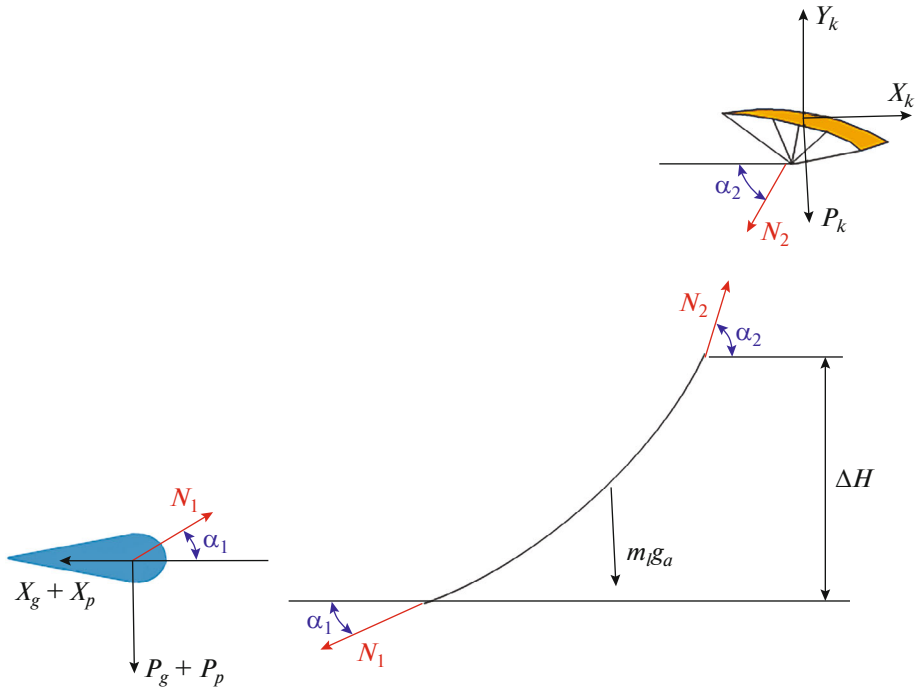

Fig. 4. Conditions for the equilibrium between the nacelle, the girtline, and the airfoil.

tion; summands two and three are determined by the chosen weight and geometric parameters of the probe.

Having found $V_{H\min}$ by the table profile of the winds or by interpolation, we determine the required altitude H for the airfoil. It should be noted that, until H is determined, the values of the atmospheric density ρ_H will be unknown. Thus H will be found by iteration in the course of design.

In addition, after H is found, it will be necessary to refine the girtline weight m_l according to the altered elevation difference.

The girtline horizontal tilt at the junction point with the nacelle is found under the nacelle equilibrium condition (Fig. 4) as

$$\tan\alpha_1 = \frac{(m_g + m_p)g_a}{(C_{Xp}S_p + C_{Xg}S_g)\rho_h \dfrac{(V_c - V_h)^2}{2}} = \frac{2(m_g + m_p)g_a}{(C_{Xp}S_p + C_{Xg}S_g)\rho_h (V_c - V_h)^2}. \quad (9)$$

Assuming that the girtline sag is below the girtline length, we derive the following system of equations from the girtline's equilibrium condition (Fig. 4):

$$\begin{cases} N_1 \cos\alpha_1 = N_2 \cos\alpha_2 \\ N_1 \sin\alpha_1 + m_l g_a = N_2 \sin\alpha_2. \end{cases}$$

Then

$$\tan\alpha_2 = \tan\alpha_1 + \frac{m_l g_a}{N_1 \cos\alpha_1} = \tan\alpha_1 + \frac{2m_l g_a}{(C_{Xp}S_p + C_{Xg}S_g)\rho_h (V_c - V_h)^2}$$

or, taking (9) into account,

$$\tan\alpha_2 = \frac{2(m_g + m_p + m_l)g_a}{(C_{Xp}S_p + C_{Xg}S_g)\rho_h (V_c - V_h)^2}.$$

The girtline length is found from Fig. 4 by very tentatively approximating the curved girtline with the circumferential arc as

$$L_l = \frac{(H - h)(\alpha_2 - \alpha_1)}{\cos\alpha_1 - \cos\alpha_2}.$$

Characteristics of the Atmosphere of Venus

The key characteristic of the external conditions that determine the vetrolet's functioning and, ultimately, its design characteristics, is the distribution of wind speeds by height.

We can currently make judgments about the atmosphere of Venus according to published findings of surveys conducted using automated interplanetary spacecraft.

According to (Svedhem, 2007), the average wind speed at a height of 70 km is 100 ± 10 m s^{-1} within a latitude range of 0 to 50 degrees. That said, the speed

Table 3. Accepted model of atmospheric density distribution by altitude

Altitude, km	Atmospheric density, kg m^{-3}
45	2.460
50	1.460
55	0.868
60	0.381
65	0.161
70	0.065

gradient by height (vertical shift) at a level of 50 km is 3 m s^{-1} km^{-1}.

Next, we shall provide the characteristics of the atmosphere of Venus according to (Sanchez-Lavega, 2008). The low latitudes of the Southern Hemisphere are characterized by zonal winds with a speed of 105 ± 10 m s^{-1} at a height of 61–66 km (top surface of the cloud layer); this speed remains constant until 55° S and then drops to zero closer to the pole (the gradient is 0.026 m s^{-1} km^{-1}). At a height of 47 km (bottom surface) the winds blow at 60–70 ± 10 m s^{-1}; then their speed drops to zero closer to the pole (the gradient is 0.021 m s^{-1} km^{-1}).

In the high latitudes, the winds blow at 15 m s^{-1} without any vertical gradient.

The meridional winds blow at 5–10 m s^{-1} (averaged for the Southern Hemisphere).

The vertical shift in the zone of 0 to 55° S at heights of 61–66 and 47–61 km is 8 ± 2 and less than 1 m s^{-1}, respectively. In the near polar regions at heights of 47–66 km the shift is 2 m s^{-1} km^{-1}.

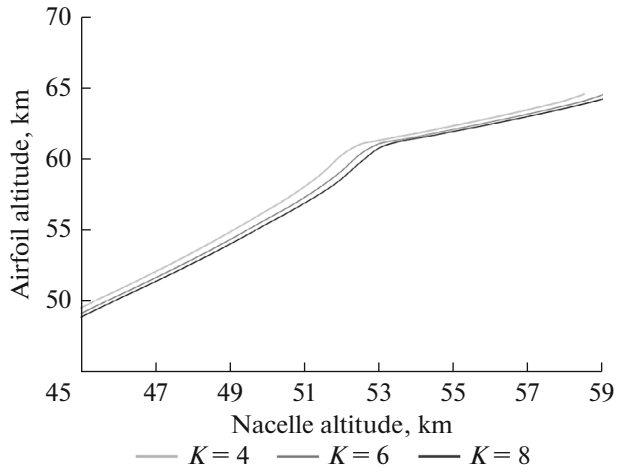

Fig. 5. Relation of the airfoil altitude to the nacelle altitude and the aerodynamic quality of the airfoil for a nacelle of 30 kg in weight (M_{nc}).

According to (Patsaeva et al., 2015), the zonal wind speed at a height of 67 ± 2 km is 90 m s^{-1} in low latitudes, and 100 m s^{-1} at 40°–50° S, and then falls to zero. The meridional wind speed varies from 0 m s^{-1} at the equator to 10–15 m s^{-1} at 50°–60° S.

According to (Hueso et al., 2008), the low-latitude zonal wind speeds are 105 m s^{-1} at heights of 47–66 km near the upper range limit and 60–70 m s^{-1} near the bottom limit. The wind speed and the shift decrease in the higher latitudes. The meridional wind at 55° S is 10 m s^{-1}.

We see that the atmosphere of Venus is characterized by a fairly complex wind speed profile by height. That is why the preliminary design research was conducted using a simplified model, the parameters of which are found in Table 2.

Another critical parameter necessary for modeling the planet's atmosphere is its density. The distribution of density used in this study relies on the data from (Petropoulos, 1988) provided in Table 3.

The consideration of the effect of the atmosphere's temperature and chemical composition goes beyond the scope of the article.

Design Calculation Results

The preliminary design calculation was made in a program written in C++ for a nacelle with M_n=30 kg in the configurations with a soft, a semirigid, and a rigid airfoil. The difference in the airfoil configuration was expressed in the respective specific weights and loads per unit area.

The variation range of the airfoil aerodynamic quality corresponded to the values typical of the given airfoil design.

The calculation results are given in Figs. 5–9. Because the article has limited scope, results are given only for the soft configuration of the airfoil for which the selected wing loading and the specific weight are ps = 3.1 kg m^{-2} and m_{spk} = 0.25 kg m^{-2}, respectively. The girtline's specific weight is m_{spl} = 1.132 kg km^{-1}, which corresponds to a Kevlar cable 1 mm in diameter.

The curve breaks in the vicinity corresponding to an altitude of more than 60 km reached by the airfoil are explained by the sharply changed wind speed profile at such heights and by a more than twofold increase in the speed gradient by height, whereas the nacelle and the braking parachute continue flying at lower altitudes with the same value of the previous velocity gradient.

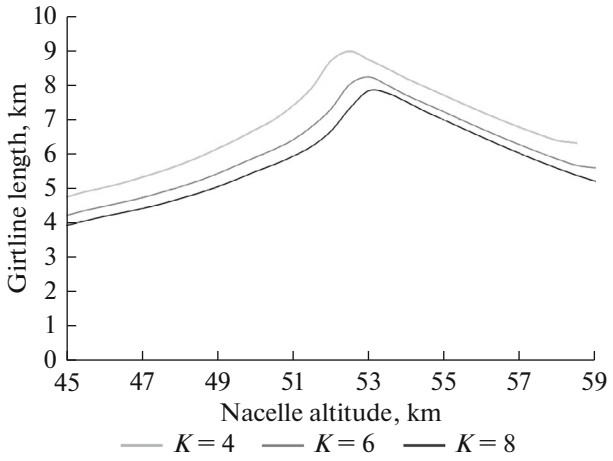

Fig. 6. Relation of the girtline length to the nacelle altitude and the aerodynamic quality of the airfoil for a nacelle with M_{nc}= 30 kg.

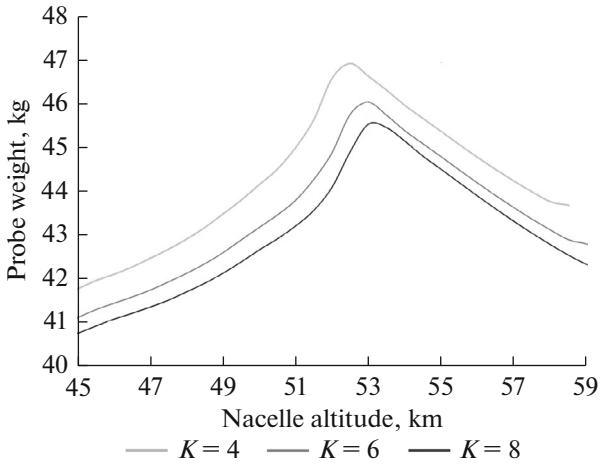

Fig. 7. Relation of the probe weight to the nacelle altitude and the aerodynamic quality of the airfoil for a nacelle of 30 kg in weight (M_{nc}).

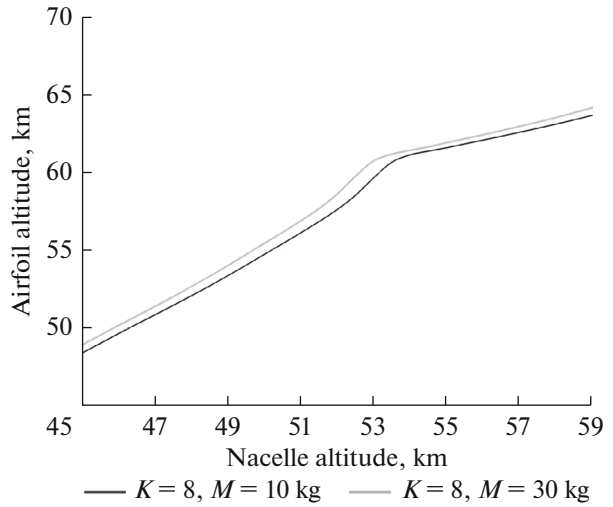

Fig. 8. Relation of the airfoil altitude to the nacelle altitude and weight at a airfoil aerodynamic quality of $K = 8$.

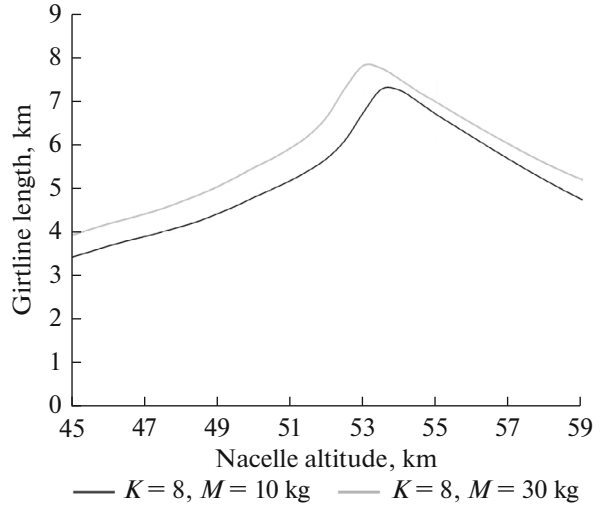

Fig. 9. Relation of the girtline length to the nacelle altitude and weight at a airfoil aerodynamic quality of $K = 8$.

CONCLUSIONS

Considering the results of the these design calculation results, it is possible to draw the following conclusions:

(1) The wind speed distribution by height and its stability over time have a critical influence on the design characteristics of the vetrolet probe. Thus, the wind profile is one of the most vital sources of data for the design process. The change in wind speed will have a decisive effect on the altitude of the probe in flight and the stability of its operation.

(2) The airfoil altitude, the probe weight, and the girtline length and tension force decrease with the increasing aerodynamic quality of the airfoil at a specified altitude. This is because the lifting force at a higher aerodynamic quality value can be generated at a weaker ram-air flow, i.e., when the airfoil is at a lower altitude.

(3) The increased load on the airfoil area increases all of the specified parameters.

(4) The rigid structure of the airfoil (glider type) implies higher loads on the area, higher specific weight, is more reliable in terms of operation but reduces the probe's mass perfection in general and requires a longer girtline.

(5) The airfoil's soft design enhances the probe's mass factor, shortens the girtline length but is much less reliable in operation.

(6) In all cases the girtline is several kilometers long, which requires solving a wide range of engineer-

ing and operational problems related to the functioning of the deployment system and to ensure the probe's general reliability and controllability.

(7) Taking account of the indicated difficulties, it makes sense to consider not only probes of this kind but also the possibility of deploying in the atmosphere of Venus airplane-type aerodynamic automated vehicles.

REFERENCES

Hueso, R., et al., The atmosphere of Venus: winds and clouds observed by Virtis/Venus Express. http://www.slac.stanford.edu/econf/C07091016/papers/LNEAIII-Hueso.pdf. Accessed April 8, 2017.

Lemeshevskii, S.A., Grafodatskii, O.S., Karchaev, Kh.Zh., and Vorontsov, V.A., Spacecrafts for the Venus contact research. Experience and trends. To the 80th anniversary of Lavochkin Research and Production Association, *Vestn. NPO im. S.A. Lavochkina*, 2017, no. 2, pp. 52–58.

Lobanov, N.A., *Osnovy rascheta i konstruirovaniya parashyutov* (Parachute: Design and Constructing Foundations), Moscow: Mashinostroenie, 1965.

Patsaeva, M.V., et al., The relationship between mesoscale circulation and cloud morphology at the upper cloud level of Venus from VMC/Venus Express, *Planet. Space Sci.*, 2015, vols. 113–114, pp. 100–108. https://mipt.ru/dppe/upload/ispavr/2015_Patsaeva.pdf. Accessed April 8, 2017.

Petropoulos, B., Physical parameters of the atmosphere of Venus, *Earth, Moon Planets*, 1988, vol. 42, pp. 29–40. doi 10.1007/BF00118037. http://articles.adsabs.harvard.edu/cgi-bin/nph-iarticle_query?1988EM%26P...42...29P &data_type=PDF_HIGH&whole_paper= YES&type=PRINTER&filetype=pdf. Accessed April 8, 2017.

Sánchez-Lavega, A., et al., Variable winds on Venus mapped in three dimensions, *Geophys. Res. Lett.*, 2008, vol. 35, p. L13204. doi 10.1029/2008GL033817. http://onlinelibrary.wiley.com/doi/10.1029/2008GL033817/epdf. Accessed April 8, 2017.

Svedhem, H., Titov, D.V., Taylor, F.W., and Witasse, O., Venus as a more Earth-like planet, *Nature*, 2007, vol. 450, pp. 629–632. doi 10.1038/nature06432. https://www.researchgate.net/publication/5802281_Venus_as_a_more_Earth-like_planet. Accessed April 8, 2017.

Vaisberg, O.L., VEGA mission: memories of the membership. To the 30th anniversary of spacecraft rendezvous with comet Halley, *Vestn. NPO im. S.A. Lavochkina*, 2016, no. 2, pp. 22–30.

Vorontsov, V.A., Krainov, A.M., Martynov, M.B., Pichkhadze, K.M., et al., Proposals on Venus research expansion by considering Lavochkin Research and Production Association researches, *Trudy Mosk. Aviats. Inst.*, 2012, no. 52. http://www.mai.ru/upload/iblock/2b6/predlozheniya-po-rasshireniyu-programmyissledovaniy-venery-s-uchetom-opyta-proektnykhraz-rabotok-npo-im.-s.a.-lavochkina.pdf. Accessed April 8, 2017.

Translated by S. Kuznetsov